INTERLAMINAR TOUGHNESS IMPROVEMENT OF CARBON FIBRE/EPOXY COMPOSITE LAMINATES BY ELECTROSPUN NANOFIBRE INTERLEAVES

M. Kuwata[1]*, H. Zhang[1], E. Bilotti[1], T. Peijs[1]

[1] *Queen Mary University of London, School of Engineering and Materials Science, and Centre for Materials Research, Mile End Road, London E1 4NS, UK*
* *m.kuwata@qmul.ac.uk*

Keywords: Interlaminar toughness, Carbon composite, Elecrospun fibres, Interleaving.

Abstract

This paper reports an interlaminar toughening concept based on nanofibre veil interleaves, which are added at the interlaminar region in a carbon fibre/epoxy laminate. The composites were prepared by resin infusion of carbon fibre fabrics using an electrospun nylon nanofibre non-woven as an interleaf between layers of carbon fabric. It was found that Mode-I fracture toughness, G_{IC} increased for thinner nanofibre veils, while thicker veils showed no improvement. It was found that the primary toughening mechanism of these electrospun nanofibre veils is by fibre-bridging during crack propagation.

1 Introduction

A major constraint on the use of laminated fibre reinforced composites continues to be their poor interlaminar toughness under both Mode-I and Mode-II loading. In practice this results in the materials suffering from a number of in-service problems. They are susceptible to impact damage from relatively low energy out-of-plane impacts which generate delamination with an associated reduction in compression strength. There are also difficulties with adhesive bonding whereby a strong bond, be it to a metal or another composite section may still exhibit unacceptable failure due to delamination close to the bond line but within the adhesive itself. Sections such as T- or H-sections created from 2-D reinforcements, such as woven fabrics, inevitably have lines of weakness resulting in stress transfer problems in structures and early failure, again by delamination.

There have been many solutions proposed to improving delamination resistance, or more precisely interlaminar toughness, by modifying the construction or constituent materials used in composites. Most of these solutions have benefits in some situations but have limitations or restrictions on where they can be used. The use of toughened matrix systems has been a major area of research and development over a thirty year period. The progressive improvement in matrix and subsequent composite toughness due to the development of formulated epoxies, rubber particle toughened epoxies, thermoplastic particle toughened epoxies, monolithic thermoplastic matrices, phase separated and phase inverted thermoplastic toughened epoxies, has proved very beneficial [1-13]. It is likely however that the limits of composite toughening

that can be achieved via bulk matrix toughening have already been reached. Excessive matrix toughening could lead to problems with *Tg*, and possibly would not be effective in a high volume fraction composite as the space for additional levels of plastic deformation within the structure is constrained. A modified approach that has been very successful is the use of tough resin interlayers or interleaves positioned between the individual laminae of the composite. This planar toughening system increases the thickness of the interlaminar region and allows the benefits of the ductile tough interlayer to be exploited [1, 14]. Interlayers of this form do however introduce weight penalties and marginally increase the thickness of the composite part. There is also the possibility that cracks can propagate by avoiding the toughened layer altogether [1]. In previous research several non-woven veil interleaved composites were investigated for Mode-I interlaminar fracture toughness [14-19]. If these are positioned between the layers of reinforcing fabrics used in an infused composite they have the potential to create interlayer toughening via fibre bridging effects. The fibres are free to migrate from the interlayer position into both the upper and lower fabric plies during the infusion and consolidation process. The role of fibre bridging in improving interlaminar toughness, especially in Mode-I is well known and well reported in the literature [20-25]. The detailed construction of the veil, its porosity, and degree of fibre entanglement and bonding is likely to influence the degree and effectiveness of any fibre bridging that might occur. The fibre in the veil can be also changed as can the diameter of the fibres and consequently the degree of bonding achieved between the veil fibres and the matrix. Finally, the veils could be constructed with a mixture of fibres, with each constituent in that mixture being varied as before, in terms of fibre diameter, length, surface condition. So far most research in the area of composite toughening using non-woven interleaves has been based on traditional micron-sized fibre mats. These relatively thick fibre mats can significantly reduce the overall reinforcement content and as such lower other mechanical properties such as strength and stiffness. Here we report the potential of thin electrospun nanofibre non-wovens as interleave materials with potentially lesser penalties to other structural properties.

2 Materials and Experiments

2.1 Materials

To investigate interlaminar toughness, twill-weave-carbon fabric was selected as the base materials. The fabric (G0986) was supplied by Hexcel Ltd., having an areal weight of 280 g/m^2 and a dry ply thickness of approximately 0.35 mm. The epoxy resin as the matrix is chosen HexFlow RTM 6-2 which is a two component resin system, also supplied by Hexcel Ltd..

2.2 Electrospun veils

Elecrospun nanofibre veil were made by Nanospider^{TM} technology for the production of nanofibre veils. The solvents used were formic acid and a combination of formic- and acetic acid. The constituents of the polyamide 6 (PA6) polymer melt prepared for the elecrospun included: 12 wt.% PA6, with 88 wt.% solvent (ratio of acetic acid to formic acid is 1:1). Conditions are 60 kV, 18 cm electrode distance, and electrode spinning at 25 Hz. Two different thickness veils were made by changing electrospinning time. The nanofibre veil thicknesses are 14 µm (Nano-veil 1) and 35 µm (Nano-veil 2). Micro fibre veil was also used in this research as a reference. Polyamide (PA) veil was supplied by Japan Vilene. Diameters of the PA6 nano-veil fibres are about 270 nm (Nano-veil 1) and 570 nm (Nano-veil 2), respectively. Fibres in the PA veil are about 37 µm in diameter. SEM images of the interleaf veils are shown in Figure 1.

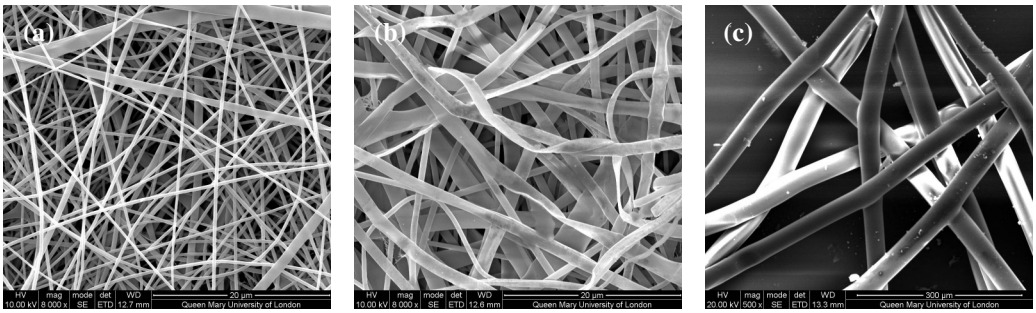

Figure 1. SEM images of non-woven interleaf veils: (a) PA6 nano veil 1 (14 µm thickness), (b) PA6 nano veil 2 (35 µm thickness), (c) PA veil (Micro fibre veil).

2.3 Composite fabrication

For interlaminar toughness test specimens, the fabrics and interleaf veils were cut into 150 mm (in length) x 150 mm (in width) rectangles. The fabrics were laid in stacks of 10 plies on the rigid mould. An interleaf veil (150 mm x 150 mm) was placed at the centre of the stack of dry fabrics prior to infusion together with a sheet of release film (A6000, supplied by Aerovac, 100 mm x 180 mm) also inserted at the mid-point (between 5th and 6th ply) to act as a starter crack in subsequent toughness tests.

During infusion processing, the resins and mould were pre-heated to 80^{o}C and 110^{o}C, respectively. After resin and hardener were mixed (mixing weight ratio is 59.5:40.5), the resin was degassed for 30 min at 80^{o}C. When degassing was finished, the resin was infused into the mould. After infusion the entire mould was placed in an oven where the temperature was programmed to increase from 30^{o}C to 140^{o}C ramping at 3^{o}C/min. When the temperature reached 140^{o}C, the oven was held at that temperature for 1.5 h. After 1st stage curing, post-curing started continuously. The post-curing temperature was set to increase from 140^{o}C to 180^{o}C ramping at 3^{o}C/min, followed by a holding step at 180^{o}C for 2 h.

2.4 Mode-I interlaminar fracture test

The Mode-I interlaminar toughness of the composites was evaluated using the double cantilever beam (DCB) test. Figure 2 illustrates schematically the DCB test specimen. The DCB specimens were rectangular in shape, 135 mm (in length) x 20 mm (in width). The test condition of the DCB test was in accordance with ASTM D5528 [26]. The DCB tests were carried out using a universal test machine (Instron 5566) equipped with a 1 kN load cell. The DCB specimens were clamped via piano hinges in the fixtures. The crosshead speed was set at a constant 1 mm/min. During loading, the load-displacement data were recorded, and the onset of delamination crack propagation was visually observed on the edge of the specimen and the crack length noted. When the crack length grew 3 to 5 mm, the specimen was unloaded. Thereafter the specimen was reloaded at the same constant crosshead speed of 1 mm/min, until the final delamination crack length increment (40 mm to 50 mm) was reached. The Mode-I energy release rates, G_I, were calculated using a modified beam theory (MBT) method [26]. The equation is:

$$G_I = \frac{3P\delta}{2b\left(a + |\Delta|\right)} \tag{1}$$

Where P is the load, δ is the load point displacement, b is specimen width, a- is the delamination length, and Δ is determined experimentally by generating a least square plot of the cube root of compliance, $C^{1/3}$, as a function of delamination length.

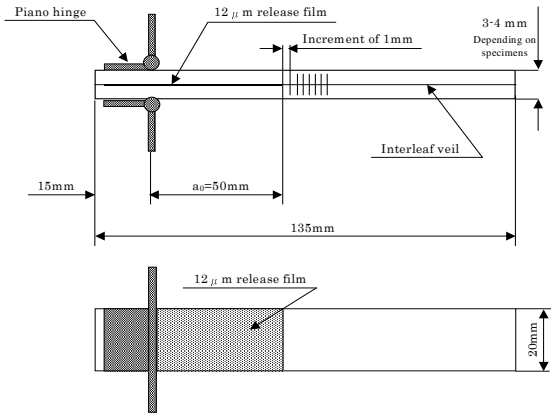

Figure 2. Geometry of DCB test sample

2.5 Scanning electron microscopy

Fracture surfaces were observed using scanning electron microscopy (SEM, FEI Inspect F). Tested specimens were cut about 10 mm in length from the crack initiation point. SEM specimens were coated with a thin layer of gold prior to observation. The acceleration voltage was 20 kV. The SEM observation was used to evaluate the suppression behaviour of crack propagation in each interleaved specimen.

3 Results and Discussion

Figure 3 shows load-displacement curves for control and interleaved samples. The curves for all specimens follow stick–slip behaviour common in composite laminates based on epoxy matrix and woven fabrics. For the PA6 Nano-veil 1 interleaved specimen, the load is significantly higher than for the reference sample. The crack for the thicker PA6 Nano-veil 2 interleaved one jumped more extensive than for other specimens. PA micro-veil interleaved samples showed the highest load of all specimens. Also crack propagation was here significantly slower than for other interleaved laminates.

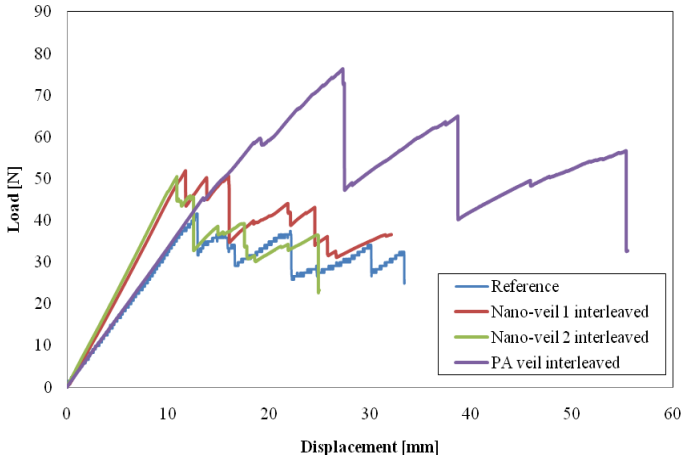

Figure 3. Representative load-displacement curves for control and nylon veil interleaved specimens

The energy release rates versus crack length for both reference and interleaved samples are shown in Figure 4. The overall trend for the Nano-veil 1 interleaved sample is almost the same as for the reference specimen. However, Nano-veil 2 interleaved samples show a

slightly lower G_I values than the control. On the other hand, the energy release rate values of the PA micro-veil specimen significantly increase to around 2 kJ/m^2.

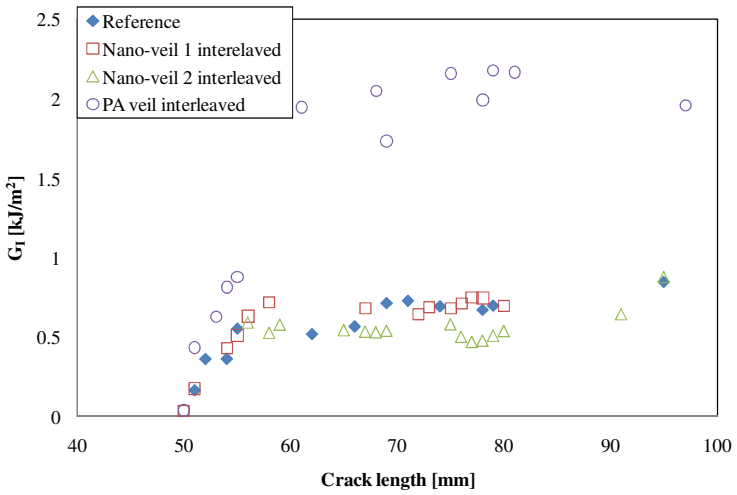

Figure 4. Resistance curves for control and nylon interleaved specimens

Critical Mode-I energy released rate values (initial and propagation), $G_{IC\text{-}NL}$ and $G_{IC\text{-}prop}$, are shown in Figure 5. The average $G_{IC\text{-}prop}$ was calculated using the propagation G_I values at different crack lengths. Both the G_{IC} values are slightly increased with Nano-veil 1. In contrast, Nano-veil 2 interleaved samples show a slightly lower G_{IC} value than the reference laminate. For PA micro-veil interleaved samples, the initial critical energy release rate values are slightly higher than the reference. The propagation energy release rate value, however, is significantly higher at about 2 kJ/m^2.

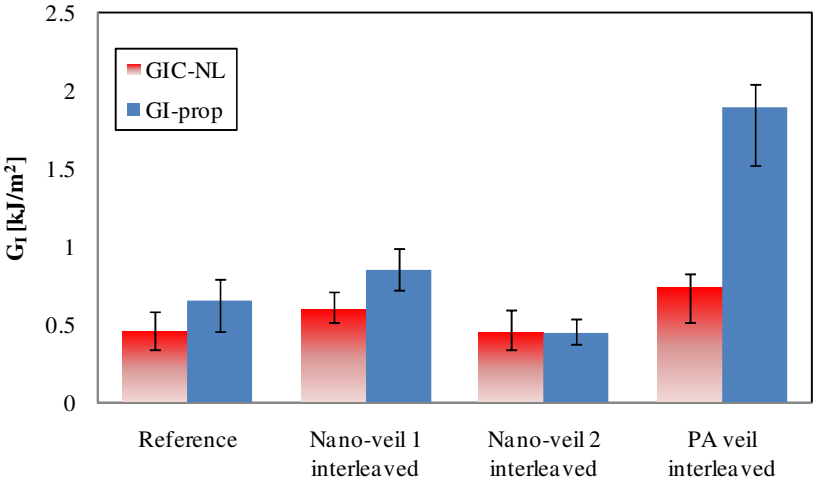

Figure 5. Mode-I initiation and propagation energy release rate values

Figure 6 shows SEM images of fracture surfaces of the DCB tested samples. These values are increased with Nano-veil 1 interleaved samples. This is evident as some debonding and pull-out of veil fibres appear on the fracture surface (Figure 6 a). These debonded fibres may lead to fibre-bridging. This bridging effect can provide toughening simply as a result of the pinning mechanism producing a stress-shielding effect on the crack tip, requiring an effective increase in global applied load to produce a further increment of crack growth. It is also conceivable that the bridging fibres can contribute to the overall toughness by absorbing

energy during crack growth as a result of plastic deformation processes in the fibres themselves. For the Nano-veil 2 interleaved sample, there is no evident fibre pulled-out of veil fibres (Figure 6 b). The thicker nano-veil fibres are here bonded to each other, as shown in Figure 1 b. The veil fibres, therefore, cannot be worked by fibre-bridging and do not improve the Mode-I interlaminar toughness. On the other hand, toughening mechanisms in the PA micro-veil interleaved samples are significantly different from other nanofibre veil specimens. PA micro-veil fibres are not visible at the fracture surface in Figure 6 c. It is believed that here the veil fibres may have melted during curing, and that the mechanism of interlaminar fracture toughness improvement could be due to thermoplastic toughening of the epoxy matrix.

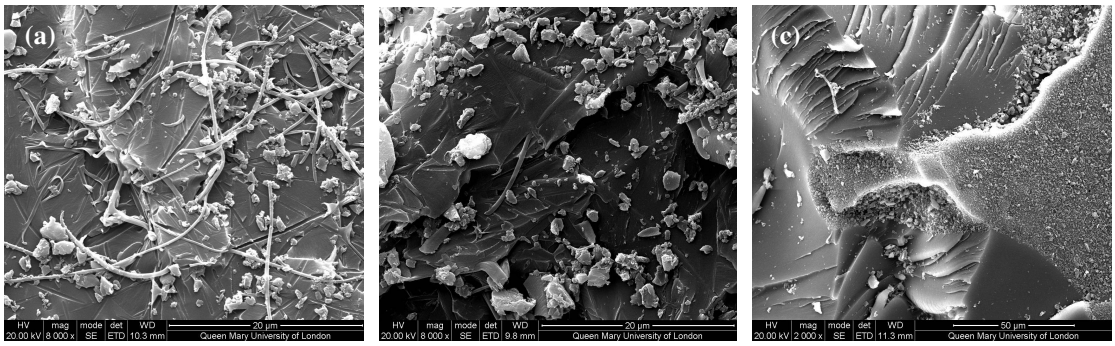

Figure 6. SEM images of fracture surface: (a) PA6 Nano-veil 1 interleave, (b) PA6 Nano-veil 2 interleave, (c) PA micro-veil interleave.

4 Conclusion

The introduction of thin electrospun nanofibre veils into a carbon fibre laminate can result in a slight increase in toughness in Mode-I interlaminar fracture toughness. The mechanism of toughening under Mode-I loading conditions is tentatively linked to fibre bridging effects that are enhanced by the introduction of the nanofibre veils. Laminates incorporating a nylon veil based on microfibres showed more significant improvements in Mode-I interlaminar toughness with the toughening mechanism, however, being completely different from the nanofibre veils.

5 Acknowledgement

We would like to acknowledge Hexcel Ltd. and Japan Vilene Company Ltd. for supplying the materials. This research work is carried out under the framework of the European Research Programme “IMS & CPS” in the Seventh Framework Programme.

References

[1] Sela N., Ishai O. Interlaminar fracture toughness and toughening of laminated composite materials: a review. *Comp*, **20**, pp. 423-435 (1989)
[2] Scott J.M., Phillips D.C. Carbon fibre composites with rubber toughened matrices. *J of Mater Sci*, **10**, pp. 551-562 (1975)
[3] Wilkinson S.P., Ward T.C., McGrath J.E. Effect of thermoplastic modifier variables on toughening a bismaleimide matrix resin for high-performance composite materials. *Polymer*, **34**, pp. 870-884 (1993)
[4] Boogh L., Pettersson B., Manson J.A.E. Dendritic hyperbranched polymer as tougheners for epoxy resins. *Polymer*, **40**, pp. 2249-2261 (1999)
[5] Mezzenga R., Boogh L., Manson J.A.E. A review of dendritic hyperbranched polymer as modifiers in epoxy composites. *Comp Sci and Tech*, **61**, pp. 787-795 (2001)

[6] Frassine R., Pavan A. Viscoelastic effects on the interlaminar fracture behaviour of thermoplastic matrix composites: II. Rate and temperature dependence in unidirectional PEI/carbon-fibre laminates. *Comp Sci and Tech*, **54**, pp. 193-200 (1995)
[7] Frassine R., Pavan A. Viscoelastic effects on the interlaminar fracture behaviour of thermoplastic matrix composites: I. Rate and temperature dependence in unidirectional PEEK/carbon-fibre laminates. *Comp Sci and Tech*, **56**, pp. 1253-1260 (1995)
[8] Davies P., Cantwell W., Moulin C., Kausch H.H. A study of the delamination resistance of IM6/PEEK composites. *Comp Sci and Tech*, **36**, pp. 153-166 (1989)
[9] von Bradsky G., Chivers R.A., Crick R.A., Turner R.M. Interlaminar fracture toughness of a range of continuous fibre PEEK composites. *Comp Sci and Tech*, **47**, pp. 75-81 (1993)
[10] Kim K.Y., Ye L. Interlaminar fracture toughness of CF/PEI composites at elevated temperatures: roles of matrix toughness and fibre/matrix adhesion. *Comp Part A*, **35**, pp. 477-487 (2004)
[11] Hashemi S., Kinloch A.J., Williams J.G. Mechanics and mechanisms of delamination in a Poly(ether sulphone) - Fibre composite. *Comp Sci and Tech*, **37**, pp. 429-462 (1990)
[12] Hine P.J., Brew B., Duckeet R.A., Ward I.M. Failure mechanism in carbon-fibre-reinforced poly(ether sulphone). *Comp Sci and Tech*, **43**, pp. 37-47 (1992)
[13] Kuboki T., Jar P.Y.B., Forest T.W. Influence of interlaminar fracture toughness on impact resistance of glass fibre reinforced polymers. *Comp Sci and Tech*, **63**, pp. 943-953 (2003)
[14] Hojo M., Ando T., Tanaka M., Adachi T., Ochiai S., Endo Y. Modes I and II interlaminar fracture toughness and fatigue delamination of CF/epoxy laminates with self-same epoxy interleaf. *Inter J Fatigue*, **38**, pp. 1154-1165 (2006)
[15] Hogg P.J. Toughening of thermosetting composites with thermoplastic fibres. *Mater Sci and Eng A*, **412**, pp. 97-103 (2005)
[16] Tzetzis D. Feasibility study on the vacuum infusion of composite to composite in-field repairs. *PhD thesis*, Queen Mary, University of London, (2003)
[17] Kuwata M., Matsuda S., Kishi H., Murakami A., Hogg P.J. Impact resistance of interleaved FRP using non-woven fabric as interleaf materials. *J of the Japan Soc for Comp Mater*, **33**, pp. 55-61 (2007)
[18] Kuwata M., Hogg P.J. Interlaminar toughness of interleaved CFRP using non-woven veils: Part 1. Mode-I testing. *Comp Part A*, **42**, pp. 1551-1559 (2011)
[19] Kuwata M., Hogg P.J. Interlaminar toughness of interleaved CFRP using non-woven veils: Part 2. Mode-II testing. *Comp Part A*, **42**, pp. 1560-1570 (2011)
[20] Hu X.Z., Mai Y.W. Mode I delamination and fibre bridging in carbon-fibre/epoxy composites with and without PVAL coating. *Comp Sci and Tech*, **46**, pp. 147-156 (1993)
[21] Suzuki T., Miyajima T., Sakai M. The role of the fiber/matrix interface in the first matrix cracking of fiber-reinforced brittle-matrix composites. *Comp Sci and Tech*, **51**, pp. 283-289 (1994)
[22] Hu X.Z., Mai Y.W. Mode I delamination and fibre bridging in carbon-fibre/epoxy composites with and without PVAL coating, *Comp Sci and Tech*, **46**, pp. 147-156 (1993)
[23] Johnson W.S., Mangalgiri P.D. Investigation of fiber bridging in double cantilever beam specimens. *J of Comp Tech & Res*, **9**, pp. 10-13 (1987)
[24] Huang X.N., Hull D. Effects of fibre bridging on G_{IC} of a unidirectional glass/epoxy composite. *Comp Sci and Tech*, **35**, pp. 283-299 (1989)
[25] Madhukar M.S., Drzal L.T. Fiber-matrix adhesion and its effect on composite mechanical properties: IV. Mode I and Mode II fracture toughness of graphite/epoxy composites. *J of Comp Mater*, **26**, pp. 936-968 (1992)
[26] ASTM D 5528-94D. *Standard test method for Mode I interlaminar fracture toughness of unidirectional fiber-reinforced polymer matrix composites* (1994)